



Thin films of lithium glasses

Alain Levasseur

► To cite this version:

Alain Levasseur. Thin films of lithium glasses. Radhakrishna, S.; Chowdari, B. V. R. Materials for solid state batteries, World Scientific, pp.119-138, 1986, 9971-5-0149-X. <hal-03895078>

HAL Id: hal-03895078

<https://hal.science/hal-03895078v1>

Submitted on 12 Dec 2022

HAL is a multi-disciplinary open access archive for the deposit and dissemination of scientific research documents, whether they are published or not. The documents may come from teaching and research institutions in France or abroad, or from public or private research centers.

L'archive ouverte pluridisciplinaire **HAL**, est destinée au dépôt et à la diffusion de documents scientifiques de niveau recherche, publiés ou non, émanant des établissements d'enseignement et de recherche français ou étrangers, des laboratoires publics ou privés.



HAL Authorization

THIN FILMS OF LITHIUM GLASSES

A. LEVASSEUR

Laboratoire de Chimie du Solide du CNRS

Université de Bordeaux I

351, cours de la Libération - 33405 TALENCE CEDEX (France).

Before approaching the lithium glasses in form of thin films the two main methods to obtain these materials will be described.

I - MAKING THIN FILMS.

FILM DEPOSITION BY EVAPORATION AND CONDENSATION IN HIGH VACUUM

Thin films of materials of such different properties as metals, halides, oxides and sulphides can be obtained in the crystalline or amorphous state by condensation of the vapour. The mechanism involved in forming the film may be a pure physical e.g. simple condensation or may also involve chemical reactions.

Evaporated films were probably first made by Faraday in 1857 when he exploded metal wires in an inert atmosphere. The deposition of metal films in a vacuum by resistance heating of platinum wires was performed by Nahrwold in 1887 and only a year later this technique was used by Kundt to produce films for measuring the refractive indices of metals. In the following period, evaporated thin films had only academic interest, although the vacuum evaporation of metal films by Pohl and Pringsheim in 1912 was performed under better developed technological conditions.

The techniques of forming thin films by condensation at very low pressures have been developed in parallel with industrial development of techniques of producing high vacua in large volumes, using pumps of very high speed and suitable cleanliness.

Films obtained by condensation alone are usually made at pressures between 10^{-6} and 10^{-8} mbar and down to the lowest values that modern vacuum technology can attain. This is combined with fast deposition rates to produce deposits in which only few foreign gas atoms are incorporated.

Of great technical importance was the discovery and development of the reactive evaporation process by Auwärter 1952 and Brinsmaid 1953. Such processes which involve a chemical reaction between evaporated constituents and the gas atmosphere are carried out mainly in the 10^{-4} mbar region with slow deposition rate. The reaction is often activated either thermally or by uv radiation or alternatively by ionic or electronic bombardment.

The industrial development of these evaporation and condensation techniques is due largely to the relative ease of obtaining either pure metal films or exact stoichiometric compound deposits of uniform thickness, because the laws which determine the phenomena at low pressure are better defined than close to or at atmospheric pressure. At very low pressures, the mean free path of the vapour atoms or molecules exceeds the usual distance between evaporation source and the substrate. Thus the substrate receives a flux of vapour which travels in straight lines with no or only very few gas/vapour collisions and the spatial distribution of the condensate obeys purely geometrical laws.

If however, the residual pressure has such a value that the source to substrate distance corresponds to the mean free path of the vapour atoms, then only 37 % of the atoms travel without collision with the residual gas molecules. At residual pressures above 10^{-3} mbar, the propagation of the evaporated atoms between source and the substrates is subject to an isotropic diffusion effect because of increasing frequency of intermolecular collisions.

The pressure of the atmosphere in which deposition is carried out optimally depends on the applied technology.

1. Evaporation

The number of atoms or molecules evaporating from a liquid or solid surface depends strongly on the temperature. As is generally known, the equilibrium vapour pressure would be obtained in a thermodynamically closed system. However, in practical evaporation, no equilibrium is obtained because the environment of the vapour source acts as a vapour sink. The evaporant atoms condense on all parts that are at lower temperature than the vapour source.

Systematic investigations of evaporation rates in vacuum have been performed mainly by Hertz, Knudsen and Langmuir. In these experiments it was found that a liquid has a specific ability to evaporate and cannot exceed a certain maximum evaporation rate at a given temperature even if the heat supply is unlimited. The theoretical maximum evaporation rates are obtained only if the number of vapour molecules leaving the surface corresponds to that required to exert the equilibrium pressure p_e on the same surface, with none returning to it.

From these experiments and considerations, the following equation for the molecular evaporation rate could be formulated :

$$dN/A \, dt = \alpha_e \{ (p_e - p_h) / \sqrt{2\pi m k T} \} \, \text{cm}^{-2} \, \text{s}^{-1}$$

dN = number of evaporating atoms

A = surface area

t = time

α_e = evaporation coefficient

p_h = hydrostatic pressure

m = atomic mass

k = Boltzmann's constant

T = temperature (Kelvin)

with $\alpha_e = 1$ and $p_h = 0$, the maximum evaporation rate is obtained :

$$dN/Adt = p_e / \sqrt{(2\pi mkT)} \text{ cm}^{-2} \text{ s}^{-1}$$

Langmuir showed that eqn. is also correct for the evaporation from free solid surfaces. Multiplying by the mass of an individual atom or molecule yields the mass evaporation rate Γ per unit area.

$$\Gamma = m dN/Adt = (m/2\pi kT)^{1/2} p_e$$

$$\Gamma = 5.84 \times 10^{-2} (M/T)^{1/2} p_e \text{ g cm}^{-2} \text{ s}^{-1}$$

M = molar mass and p_e is given in torr.

The mass evaporation rate Γ is for most element of the order of $10^{-4} \text{ g cm}^{-2} \text{ s}^{-1}$ at $p_e = 10^{-2} \text{ mbar}$.

Graphs of the equilibrium vapour pressure as a function of temperature for some elements are given on fig. 1.

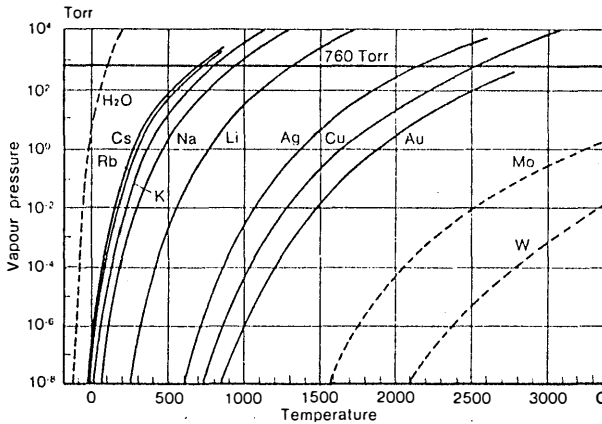


FIG. 1
Vapour pressures of some elements.

As can be seen on Fig. 2 the cross section in the symmetry axis of the spherical segment shows a sickle-shaped geometry of the deposited thin film.

a) Evaporation techniques

There are various methods for performing evaporation. However, for many materials there is only one optimum evaporation technique.

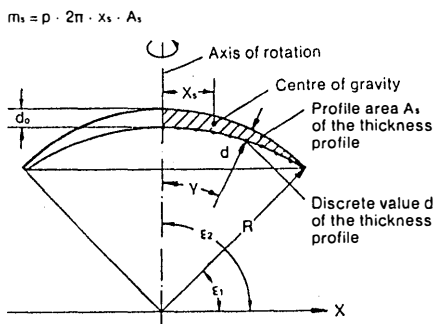


FIG. 2
Deposited film mass m_s on a spherical segment.

Principally, this concerns the correct choice of evaporation method, the evaporation source and the evaporation temperature. The technique to be applied depends primarily on the material used and the required film purity, but of course in practice also on the existing plant and installations.

The most important technique is the indirect resistance heating. The evaporation material is placed in a container made of Mo, Ta, W or C which can be in the form of a boat crucible, coil or strip. In some cases ceramic crucibles or inserts are also employed made of Al_2O_3 , BeO or BN. The container is heated by current flow and the material is evaporated or sublimed from this various types of resistance-heated evaporation sources which are shown in Fig. 3.

Other methods could be employed like electron beam heating, laser heating, high frequency heating.

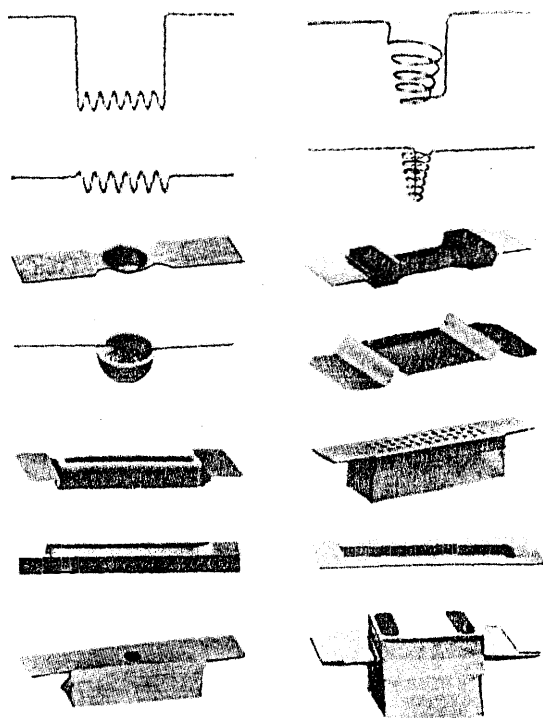


FIG. 3
Various types of resistance heated evaporation sources.

b) Condensation and film formation

In condensation, there exists a relation between a critical deposition rate and the substrate temperature. An incident vapour atom has a certain retention time on a surface which is proportional to the inverse substrate temperature and the binding forces. Some atoms are reflected, which means that an atom leaves the surface by a process which is the direct result of the collision of the atom against the surface. However, this effect will normally only be observed with substrates held at room temperature when the binding forces between the condensed atoms and the substrate are very weak and the energy of the arriving evaporated atoms is relatively low, for instance with Zn and Cd on glass. If, however, the number of the condensing Zn or Cd atoms per second is very high, few but large nuclei are formed. The condensation can be improved by pre-deposition with small amounts of other metals, such as Ag or Cr.

Formation of a solid film by condensation is generally an irreversible process. A certain dwell time on the substrate and surface diffusion processes of the atoms are responsible for nuclei formation. Heterogeneous nucleation is important as the first step in the formation of a thin film by deposition from the vapour phase.

For example Fig. 4 shows a schematic representation of the stages of metal film.

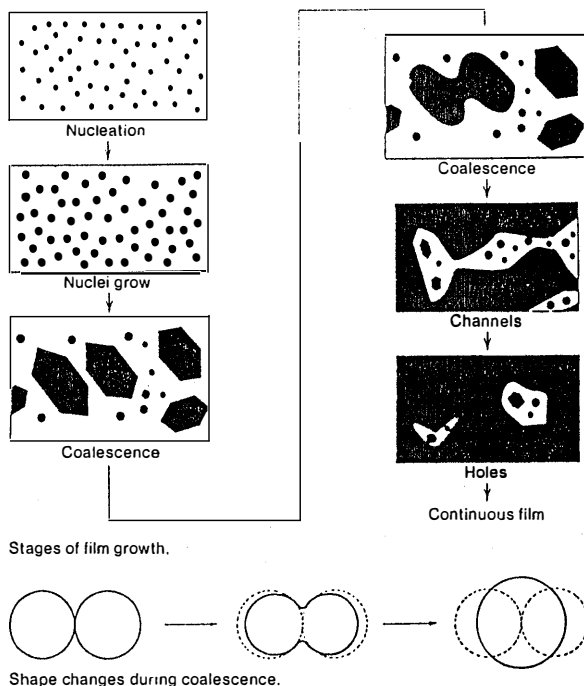


FIG. 4
Schematic representation of the stages of metal film growth and approximate relationship between dislocation density and film thickness according to Pashley.

Most films deposited even at room temperature are in a non-equilibrium state and highly imperfect containing vacancies, dislocations, stacking faults and grain boundaries, unless there is some mechanism for achieving equilibrium. The method of approaching equilibrium is by movement of atoms in and on the surface layers. The most important parameter controlling the mobility of atoms in a solid film

is diffusion. Therefore if the condensation process occurs closer to the melting point of the film material, a better ordered solid film is formed. This can be achieved, for example, by increasing the substrate temperature. In addition to influencing surface mobility and ordering processes, the substrate temperature will also affect the grain size.

c) Reactive evaporation

For the deposition of a stoichiometric oxide film by reactive evaporation, a relatively high O_2 partial pressure and a slow metal-atom condensation rate are required, so that completely oxidized metal-oxide films can be formed. The partial pressure of the reactive gas component is usually few 10^{-4} mbar. The significant technology of reactive evaporation is applied in all cases where direct evaporation of a chemical compound is not possible because of thermal dissociation or too low a vapour pressure. In practice, oxide films are usually produced using sub-oxides or metallic starting materials. However, basically it is also possible to produce sulphides and nitrides or other compounds in this manner.

2. Film deposition by cathode sputtering

Cathode sputtering or more exactly the sputtering of (usually solid) materials by bombardment with positive noble gas ions is the oldest vacuum process for producing thin films. Sputtering, the cause of the erosion of the cathode in glow discharge, often an undesirable effect, was discovered more than 130 years ago by Grove 1852 in England and Plücker in Germany during gas discharge experiments.

Soon afterwards in 1877, metal sputtering was applied in the production of mirrors and later it was used for decorating various articles with noble metal films. Around 1930 it was used for applying electrically conducting films of gold onto the wax masters of the Edison phonographs. It then became of less importance for the next 30 years compared with the rapidly developing deposition of films by evaporation and condensation in high vacuum.

However, since about 1955 sputtering has undergone a renaissance. Intensive studies of the phenomena occurring during the sputtering process and hence better control of the process together with the technical requirement for high quality films having very good adhesion and possessing specific properties have certainly contributed to the wide application.

3. General considerations

Without going into detail, we will attempt to discuss the parameters and system components of significance for cathode sputtering, and thus give a general idea of the fundamental correlations of cathode sputtering and also of the opportunities offered by this process.

Fig. 5 shows a schematic drawing of a greatly simplified set-up for cathode sputtering. The process takes place in a vacuum chamber, which has been evacuated as well as possible before coating. In order to prevent contamination of the films to be produced by incorporation of less defined residual gas, the starting pressure should be 10^{-6} mbar or lower. The working pressure is then achieved with the working gas. The sputtering process itself takes place in a gas discharge which is ignited at a pressure between 10^{-3} and 10^{-2} mbar, depending on the special variant of the method. A requirement of the vacuum pumps is therefore an ultimate vacuum as high as possible and also a high and constant pumping speed in the mbar range. These requirements are met by diffusion pumps or even better by cryopumps and by turbo molecular pumps which are also usually applied in practice. In order to maintain the gas discharge, a gas inlet, for instance in the form of a needle valve, has to be provided. The process, itself, runs on a flow-through principle. Noble gases, usually argon, are used as the working gas. However, for special applications, almost any other gases and gas mixtures can be used.

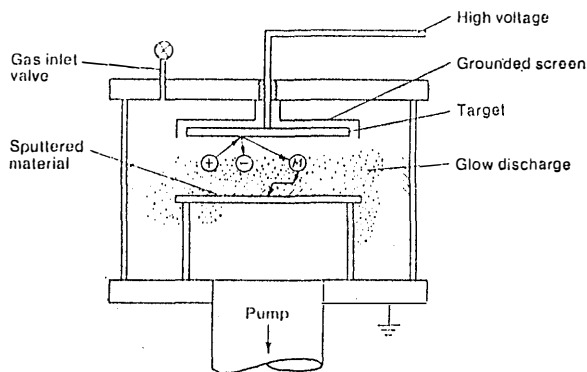


FIG. 5
Simple diode type sputtering system.

Two electrodes are installed in the chamber, one of them the so-called target serves as material source for the films to be produced and is at a high negative potential. A substrate holder is situated opposite the target, which can be earthed or applied to a floating potential. Furthermore, this holder can be heated or cooled. The positive ions produced in the gas discharge are then accelerated to the negative target. Upon bombardment of the target, they cause ejection of mainly neutral particles by impulse transfer phenomena. The ejected particles wander through the working gas and condense on the substrate. The energy range of the ions is usually between 10 and 5000 eV. A significant part of cathode sputtering is accordingly the bombardment of a solid surface with energetic particles about 1 nm per 1 keV ion energy. The process of material erosion in the sputtering process is definitely determined by momentum transfer of the impinging ions on the atoms of the upperlayers of the lattice of the solid material, and has a faint resemblance to the behaviour of billiard balls. This was soon assumed, but could be confirmed only relatively late. The process is schematically shown in Fig. 6.

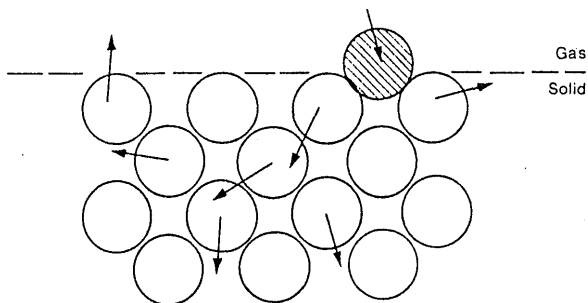


FIG. 6
Collision cascade in a solid material during ion bombardment with ejection of two atoms.

In the areas near the surface of the solid target, various complicated processes occur simultaneously. These are :

- * knocking out of neutral atoms, compounds or fragmented species,
- * secondary electron emission,
- * ejection of positive and/or negative secondary ions,
- * temperature increase,
- * emission of radiation,
- * chemical reactions and dissociation,
- * implantation, solid state diffusion, crystallographic changes,
- * reflection of incident and emitted particles.

All of these processes take place, both at the target and at the substrate and determine the properties of the growing films. About 95 % of the energy of the bombarding ions on the target is lost as heat in the solid material and only 5 % is passed onto the secondary particles.

With this technique the deposition rate is generally low (20-100 Å/mn) but the thin film clings perfectly to the substrate. It is the main advantage of this technique.

II - ELABORATION OF LITHIUM THIN FILM GLASSES

A. Binary B_2O_3 - Li_2O glasses

B_2O_3 - Li_2O thin films have been prepared using a vacuum evaporation process (10^{-7} torr).

Glasses in form of small lumps have been molten in a molybdenum boat at $600^\circ C$. Thin films (1 to 4 μm thick) have been formed on a substrate heated at $250^\circ C$. The deposition rate, controlled by a piezoelectrical balance, was 2000 $\text{\AA}/\text{min}$. After deposition, the substrate was progressively cooled with a $2^\circ C/\text{min}$. rate to avoid internal strains.

B. Ternary B_2O_3 - SiO_2 - Li_2O , B_2O_3 - Li_2O - LiI and B_2O_3 - Li_2O - Li_2SO_4 glasses

It had been previously shown that on one hand the addition of SiO_2 to B_2O_3 - Li_2O bulky glasses allows to increase the Li_2O content and hence the conductivity on the other hand that a lithium salt (e.g. LiI or Li_2SO_4) added to B_2O_3 - Li_2O glasses has a similar influence on the Li^+ conductivity.

For these glasses, a vacuum evaporation process was inappropriate. For borosilicate glasses, the vapour pressure is still very low at $1000^\circ C$. In the case of the halogenoborates, there is a large difference in the vapour pressures of LiI and of the other components : LiI evaporates at about $400^\circ C$. Li_2SO_4 in B_2O_3 - Li_2O - Li_2SO_4 glasses gets decomposed when they are heated in high vacuum. These unfavorable conditions do not allow formation of homogeneous thin films. To overcome this difficulty r.f. sputtering has been used.

A bulky glass disc (of 50 mm diameter and 3 or 4 mm thickness) was used as a target. R.f. sputtering deposition was carried out under 10^{-2} torr argon pressure and with a power of $8 \text{ W}/\text{cm}^2$ on a substrate at room temperature. The distance between target and substrate was about 50 mm. Films of 1 or 2 μm thickness have been deposited with a rate of 40 $\text{\AA}/\text{min}$.

1. Thin film characterization

X-ray diffraction analysis has shown that the films obtained are amorphous, whatever the deposition method used.

Electrical measurements.

A sandwich structure has been obtained by successive deposition of gold and glass (Fig. 7). The geometrical arrangement was realized using several masks.

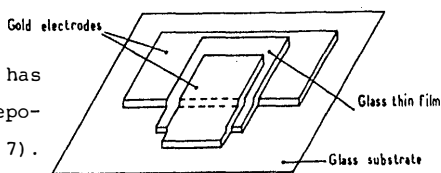


FIG. 7
Glass thin film sample between
two gold electrodes.

Ionic conductivity was measured by a classical complex impedance method using a SOLARTRON 1170 frequency pulse analyser in the frequency range of 0.1 mHz up to 10^4 Hz.

D.c. measurements were in good agreement with those obtained by a.c. and showed that the electronic conductivity is at least 10^5 times lower than ionic conductivity.

For all compositions considered plots of $\log \sigma$ against $1/T$ show a linear variation in the temperature range of the measurements (25-300°C).

In other words the conductivity data fit well with an Arrhenius equation.

a) B_2O_3 - Li_2O films

A sufficient amount of glass can be obtained by the evaporation process to allow a chemical analysis. As expected the lithium content in the amorphous films is higher than in the starting material (Fig. 8).

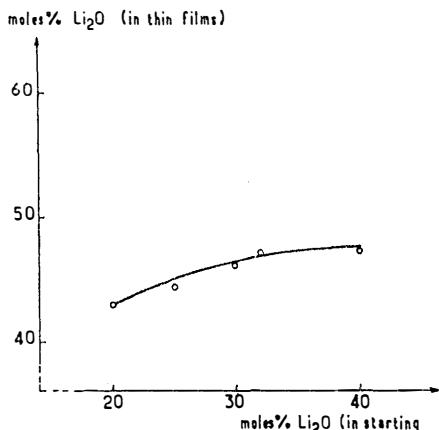


FIG. 8
Variation of Li_2O content
(in moles %) in the thin films with
 Li_2O content in the starting glasses.

Figure 9 shows the variation of $\log \sigma$ for B_2O_3 - Li_2O glasses with Li_2O content at 25°C. Conductivity values obtained with thin films fit well with those determined for bulky materials.

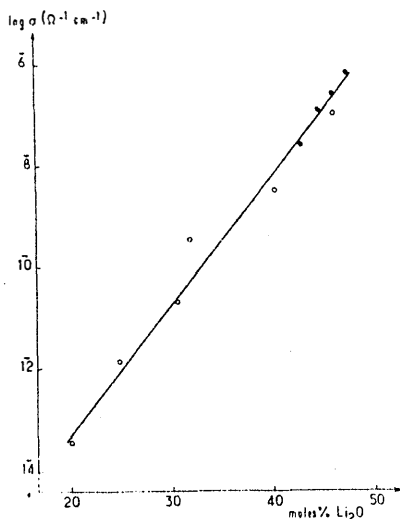


FIG. 9
Variation of $\log \sigma$ of B_2O_3 - Li_2O
glasses (o : bulky glasses ;
• : thin films) with Li_2O content
at room temperature.

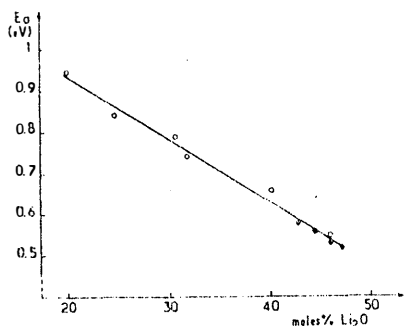


FIG. 10
Variation of the activation energy of
 B_2O_3 - Li_2O glasses
(o : bulky glasses ; • : thin films)
with Li_2O content.

A similar phenomenon is observed for the activation energies (Fig. 10).

The ionic conductivity varies exponentially with Li_2O content and the activation energy varies linearly with Li_2O content (Fig. 9, 10). Similar behavior had already been observed for glasses



belonging to the $\text{SiO}_2\text{-Na}_2\text{O}$ and $\text{M}_2\text{O}_3\text{-Li}_2\text{O}$ ($\text{M} = \text{Al}, \text{Ga}, \text{Bi}$) systems.

A scanning electron micrograph of a thin film shows a surface which is quite uniform (Fig. 11).

FIG. 11
Scanning electron micrograph of a
 $\text{B}_2\text{O}_3\text{-Li}_2\text{O}$ thin film.

b) $\text{B}_2\text{O}_3\text{-SiO}_2\text{-Li}_2\text{O}$, $\text{B}_2\text{O}_3\text{-Li}_2\text{O-LiI}$ and $\text{B}_2\text{O}_3\text{-Li}_2\text{O-Li}_2\text{SO}_4$
glasses

It is difficult to obtain an amount of material large enough using r.f. sputtering for an efficient chemical analysis. However, qualitative energy dispersion analysis using a TRACORE NORTHEM TN 1705 apparatus coupled with S.E.M. showed the presence of elements of starting ternary glasses in the corresponding thin films.

Electrical measurements seem to show that the thin film conductivity is similar to that observed in the starting bulky glasses as far as the composition of starting material and amorphous sputtering deposit does not change.

The best results have been obtained for borosilicate glasses. A $10^{-6} \Omega^{-1} \text{cm}^{-1}$ room temperature conductivity allows to attain a low electrical resistance (100Ω for $1 \mu\text{m}$ thickness and a 1cm^2 at 25°C).

This type of glasses has been used for setting up microbatteries.

C. Binary B_2S_3 - Li_2S and ternary B_2S_3 - Li_2S - LiI glasses

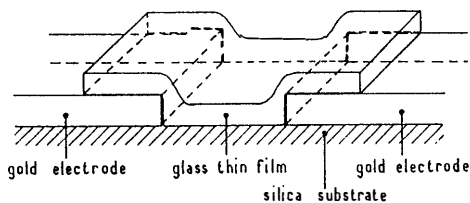
B_2S_3 - Li_2S and B_2S_3 - Li_2S - LiI thin films have been prepared using a high vacuum evaporation process (10^{-7} torr).

The starting materials and the obtained thin films are very hygroscopic. The deposition of such glasses requires a small evaporation apparatus, which has been designed and built up in order to be put easily into a glove box. This glove box is equipped with water vapor and oxygen purification devices.

The deposition rate controlled by a piezoelectrical balance is about 140 \AA s^{-1} , five times higher than that determined with oxide glasses. The obtained films are checked by SEM.

1. Electrical measurements

The high ionic conductivity of the glasses does not allow using a sandwich electrode structure for electrical measurements.

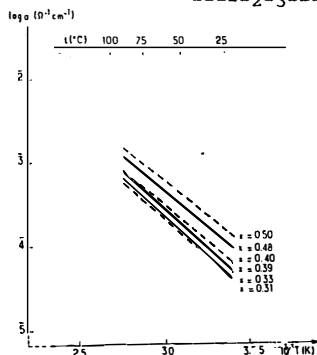


The arrangement of the electrodes used for ionic and electronic conductivity measurements of B_2S_3 - Li_2S and B_2S_3 - Li_2S - LiI thin films is illustrated in fig. 12.

The Au/thin film/Au cell is kept in a special air-tight container during the electrical measurements.

FIG. 12
Arrangement of the electrodes for electrical measurements.

a) The B_2S_3 - Li_2S binary system



The conductivity measurements show that the thin film and the corresponding starting glass have similar conductivities (Fig. 13). The ionic conductivity of this kind of glasses varies exponentially with Li_2S content. Similar behavior had been observed for oxide glasses.

FIG. 13

Variation of $\log \sigma$ vs $10^3 T^{-1}$
for $(1-x)B_2S_3-xLi_2S$ glasses

(dotted lines : thin films,
broken lines : bulky glasses).

b) The B_2S_3 - Li_2S - LiI ternary system

For B_2S_3 - Li_2S - LiI films the conductivity measurements show two types of behavior according to the thermal treatment of the thin films :

- during the first temperature increase from 25 to 90°C the measured conductivity is similar to that of the starting glasses (Fig. 14). This conductivity is due essentially to the motion of the ions in the bulk of the thin film. Thus despite the uncertainty of the exact iodine content the films seem to have the same composition and the same behavior as the starting glasses.

- the ten times higher conductivity measured when the films are heated for several hours at 90°C seems to be independent of the composition of the thin films (Fig. 14). Such a type of annealing never produces any conductivity enhancement on similar composition bulky glasses.

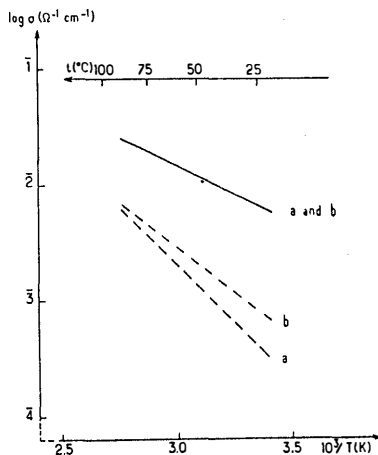


FIG. 14
Variation of $\log \sigma$ vs $10^3 \cdot T^{-1}$
for B_2S_3 - Li_2S - LiI glasses
(broken lines : thin films and
starting materials ; dotted
lines : thin films after
thermal treatment)
a : $0.14B_2S_3$ - $0.45Li_2S$ - $0.41LiI$
b : $0.14B_2S_3$ - $0.40Li_2S$ - $0.46LiI$.

This enhancement may be attributed to an interfacial conductivity due to rapid ion transport at the core of the silica-film interface. The structural defects at the interface may be responsible for the low interfacial migration enthalpy as thermal treatment increases the fraction of interfacial sites concerned.

Microbatteries

Miyauchi et al prepared microbatteries following the subsequent procedure.

- (i) Titanium disulfide cathode film was fabricated on a silica glass substrate by low pressure CVD using $TiCl_4$ and H_2S as a source gas.
- (ii) Solid electrolyte $Li_{3.6}Si_{0.6}P_{0.4}O_4$ amorphous film was rf-sputtered on the TiS_2 cathode film at a pressure of 3 Pa, using $Li_{3.6}Si_{0.6}P_{0.4}O_4$ powder and Li_2O pellets as a target, and a gas

mixture of $\text{Ar}/\text{O}_2 = 60/40$ as a sputtering gas. The substrate temperature was kept below 100°C to avoid oxidation of the TiS_2 film.

- (iii) Finally, Li anode film was vacuum evaporated at a pressure of 10^{-4} Pa.

Performance of thin film cells.

Discharge and charge curves for cell (A) and cell (B) at $3\text{--}16\ \mu\text{A}/\text{cm}^2$ are shown in Fig. 15. The open circuit voltages for both cells were 2.5 V. The prompt drop in voltage in the initial stage is due to ohmic polarization. A gradual decrease follows that is due to discharge. These discharge curves were similar to those for a TiS_2 cathode in organic solvent electrolyte cells. The discharge capacities of cell (A) from 2.5–1.5 V at $3\ \mu\text{A}/\text{cm}^2$ and $6\ \mu\text{A}/\text{cm}^2$ were about $45\ \mu\text{Ah}/\text{cm}^2$. These capacities were about 80 % of the theoretical value for TiS_2 single crystal. The discharge capacity of cell (B) at a $3\ \mu\text{A}/\text{cm}^2$ current density was $150\ \mu\text{A}/\text{cm}^2$, which was about 80 % that of the theoretical value. This increase in discharge capacity was caused by an increase in D_{Li} and thickness. There was no distinct difference between the discharge and charge curves other than the potential drop caused by internal resistance. This indicates sufficient reversibility for these cells

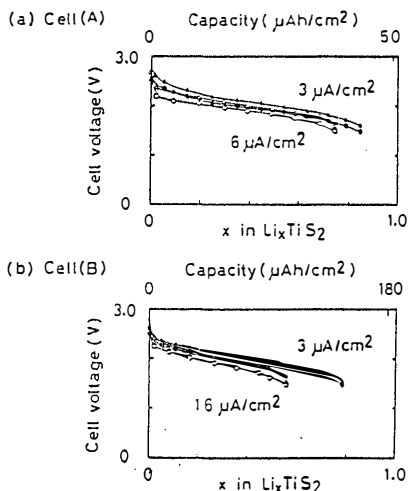


FIG. 15
Discharge and charge curves of thin
films cells
(o, o : discharge ; Δ , Δ : charge).

REFERENCES

- Coating on glass.
H.P. PULKER, Elsevier, Amsterdam (1984).
- A. LEVASSEUR, M. KBALA, P. HAGENMULLER, G. COUTURIER and Y. DANTO
Solid State Ionics, 9 & 10 (1983) 1439.
- M. KBALA, M. MAKYTA, A. LEVASSEUR and P. HAGENMULLER
Solid State Ionics, 15 (1985) 163.
- K. KANEHORI, K. MATSUMOTO, K. MIYAUCHI and T. KUDO
Solid State Ionics, 9 & 10 (1983) 1445.
Solid State Ionics, 9 & 10 (1983) 1469.